Improved image quality for x-ray CT imaging of gel dosimeters

M B Kakakhel[1, 2] **T Kairn**[3], **J Kenny**[3,4], **J V Trapp**[1,a]

[1] Faculty of Science and Technology, Queensland University of Technology, GPO Box 2434, Brisbane, Qld 4001, Australia
[2] Department of Physics and Applied Mathematics, PAM, Pakistan Institute of Engineering and Applied Sciences, PO Nilore, Islamabad, Pakistan
[3] Premion, The Wesley Medical Centre, Suite 1, 40 Chasely St, Auchenflower, Qld 4066, Australia
[4] Australian Clinical Dosimetry Service, Yallambie, Vic 3085, Australia

Corresponding Author

J V Trapp

Physics
Faculty of Science and Technology
Queensland University of Technology
GPO Box 2434, Brisbane, QLD, 4001, Australia
Phone: +61(0)731381386, Fax +61(0)731389079
E-mail: j.trapp@qut.edu.au

Abstract

Purpose: This study provides a simple method for improving precision of x-ray computed tomography (CT) scans of irradiated polymer gel dosimetry. The noise affecting CT scans of irradiated gels has been an impediment to the use of clinical CT scanners for gel dosimetry studies.

Method: In this study, it is shown that multiple scans of a single PAGAT gel dosimeter can be used to extrapolate a 'zero-scan' image which displays a similar level of precision to an image obtained by averaging multiple CT images, without the compromised dose measurement resulting from the exposure of the gel to radiation from the CT scanner.

Results: When extrapolating the zero-scan image, it is shown that exponential and simple linear fits to the relationship between Hounsfield unit and scan number, for each pixel in the image, provides an accurate indication of gel density.

Conclusions: It is expected that this work will be utilised in the analysis of three-dimensional gel volumes irradiated using complex radiotherapy treatments.

Key words: Gel dosimeter, gel dosimetry, CT imaging, SNR, Zero-scan image, radiotherapy, polymer gel

I. INTRODUCTION

Gel dosimeters, consisting of a radiation sensitive material infused in a 3D gel matrix, are increasingly being investigated for radiotherapy dose verification and quality assurance.[1] When a volume of gel is irradiated, the radiation sensitive material undergoes a measurable change in the magnetic relaxation, density and optical density which is directly related to the radiation dose received, potentially providing a high-resolution three-dimensional measurement of the dose absorbed by the gel.[2-21]

An important consideration for any dosimeter prior to clinical use is the spatial resolution and the accuracy in the measurement of the absorbed dose and many authors have investigated gel dosimetry as a solution.[2-7]

One of the challenges in gel dosimetry is the extraction of the dose information once the gel has been irradiated. Various techniques have been employed for gel dose readout including magnetic resonance imaging (MRI) [11-13], optical CT scanning (OCT) [15-16]; X-ray computed tomography (CT) [20-21], and ultrasound[16]. In MRI imaging of polymer gel dosimeters the spin-spin relaxation rate (R_2) is used to determine the radiation induced polymerization corresponding to the absorbed dose.[11-13] One issue with MRI imaging is that artefacts are significant issues affecting the accuracy of the gel dosimeters, which requires careful selection of scanning parameters to ensure accuracy.[14]

OCT has been demonstrated as viable readout technique for polymer gel dosimeters due to a post-irradiation change in optical desnisty.[15-16]; however this technique is susceptible to artefacts due to refraction of light[18-19]. Ultrasound imaging [16] utilizes changes in acoustic speed of propagation, absorption and attenuation which vary with radiation induced polymerization.

CT has been employed to exploit post irradiation changes in linear attenuation coefficient in polymer gel dosimeters.[20-26] The availability of CT scanners in radiotherapy centres makes this imaging technique attractive as a routine technique for imaging of gel dosimeters. However, the small changes in gel density arising from radiation exposure means that this technique suffers from a low signal to noise ratio (SNR). Attempts to reduce stochastic noise by averaging several CT images result in an additional dosing of the gel.[20,21] An alternative approach for the reduction of noise in CT imaging of polymer gel dosimeters has been the application of image processing techniques. [24,27,28]

The aim of the current work is to investigate the feasibility of a simple image analysis technique whereby data from multiple scans is used to provide a hypothetical 'zero-scan' image representing the irradiated gel prior to CT scanning. A simple example of a normoxic polymer gel irradiated to a range of doses is used to establish that this method is capable of appreciably improving CT image quality.

II. METHODS AND MATERIALS

II.A. Gel Preparation and Irradiation

A PAGAT gel dosimeter was prepared as described by Venning *et al*.[29] with 8 mM of Tetrakis (Hydroxymethyl) Phosphonium Chloride (THPC) for improved stability.[30] The gel dosimeter was prepared under normal atmospheric conditions and poured into a cylindrical Polyethylene terephthalate (PET) container of 10 cm height and 5 cm radius. It was then stored at 4^{o}C for 24 hrs before irradiation. The gel dosimeter was irradiated with three small (1.5 cm x 1.5 cm) fields of 118, 233 and 384 cGy parallel to the central axis of the container with a Varian linear accelerator using a 6 MV photon beam at 600 MU/min. A further 686 cGy was delivered using a fourth test field, close to the centre of the container. The area of this high-dose field was reduced to 1.0 cm x 1.0 cm to minimise possible scatter into the other test regions of the gel.

II.B. x-ray CT imaging

One day after irradiation, the gel was imaged using a GE Lightspeed RT 4 CT scanner. The CT scans used an x-ray tube load of 300 mA with 1s rotation, beam energy of 120 kVp, 5 mm slice thickness, image size of 512x512 and 25 cm field of view. The CT dose from this protocol is estimated as 83.4 mGy per scan at the scan centre, based on the ImPACT $CTDI_{100(soft\ tissue)}$ (ImPACT CT Patient Dosimetry Calculator V1.0, ImPACT, London, UK). The gel was scanned 360 times at a single slice location while placed in a cylindrical water tank similar to that described by Trapp *et al.*[21] The gel was positioned in the tank such that the CT scanning plane was orthogonal to the radiation beam direction. All scans consisted of one slice only, with no couch motion, providing a transverse image of the phantom showing all four irradiated regions at a depth of 4 cm from the surface onto which the radiation was incident. An additional set of 60 scans of the tank were obtained, with the gel removed such that the tank only contained water.

II.C. Image Analysis

The CT images, in DICOM format, were imported into Matlab (version 7.8.0.342, The MathWorks, Natick, MA, USA). The 60 images of the water phantom were averaged to reduce random noise.[21] This averaged water image was then subtracted from each of the gel images, to remove CT artefacts from the gel images, as described by Trapp *et al*.[21]

Three composite data sets were then obtained from the processed CT images, using the following method. For each pixel, the Hounsfield unit (HU) was acquired sequentially from the series of 360 processed CT images to form a data set of 360 data points for each gel voxel. For each dataset linear, quadratic (a least squares fit with the inbuilt *Polyfit* Matlab function) and exponential fits (using the ezfit function from the ezyfit curve fitting toolbox based on Matlab's built-in FMINSEARCH function (Nelder-Mead method)) were applied to the data. Thus, estimates of the relationship between scan number and HU for each voxel were obtained using Eq. (1-3):

$$HU(i,j) = L_1(i,j)N + L_0(i,j) \quad (1)$$

$$HU(i,j) = Q_2(i,j)N^2 + Q_1(i,j)N + Q_0(i,j) \quad (2)$$

$$HU(i,j) = E_o(i,j) + (A(i,j) * \mathrm{e}^{-N/B(i,j)}) \quad (3)$$

where N is the scan number and the arrays $L_n(i,j)$, $Q_n(i,j)$ and $E_n(i,j)$, $B_n(i,j)$ and $A_n(i,j)$ are free parameters for the linear, quadratic and exponential fits respectively, evaluated for each pixel (i,j). A new image was then constructed, referred to here as the zero-scan image, whereby each pixel in the new image is the intercept of the fit for the corresponding pixel in the processed CT images, i.e. the zero-scan images are maps of $L_0(i,j)$, $Q_0(i,j)$, $E_0(i,j)$ and $A(i,j)$. The rationale behind this technique is that the intercept of the fitted data most closely matches the properties of the gel dosimeter immediately before CT scanning commences.

In each of these three new images, four regions of interest (ROIs) were selected; each consisting of 121 pixels centred at the location of the 118, 233 and 384 and 686 cGy fields. One ROI was also selected corresponding to an un-irradiated region in the gel container. To provide measurements of the signal and noise in the images, the mean HU value and the standard deviation were calculated for these selected ROIs.

An analysis was also carried out to find out the optimum number of CT scans required for reconstructing the zero-scan image. Starting from the first 50 images and subsequently adding images up to 300 the average percentage error was calculated for each group of CT images. As a first step the linear reconstructed image using all the 360 scans was considered as the standard image. For each of the four ROI's described above the mean HU value was calculated and compared with the standard image, and the percentage error was calculated for each ROI. In the final step all the individual % errors in the four ROI's were averaged out and a single averaged percentage error was calculated for each group of CT images.

III. RESULTS

III.A. Qualitative

In Fig. 1 three sets of zero-scan images are shown, constructed from sets of all 360 images, the first 50 images, and the first 16 CT images respectively. The relatively poor signal to noise affecting un-processed CT scans of dosimetric gels is apparent in Fig. 1(a) top left and top middle panels , which show the first and last of the 360 CT images of the gel dosimeter series (with the averaged water image subtracted). Both images are windowed to the same pixel values and an overall increase in HU is evident, above noise, in the overall lighter appearance of Image 360. The source of this increase in HU is the gel density increase due to the radiation dose delivered during the CT imaging. Fig. 1(a) top right panel shows an average of all of the CT images of the gel dosimeter, and a reduction of noise compared to the single images can clearly be seen. Lower left, middle and right panels show the zero-scan images created from exponential, linear and quadratic fits to the data as described in Section II.C. A reduction of noise compared to the upper panels is clearly evident.

Fig. 1(b) and 1(c) show results where only the first 50 and first 16 images of the dataset respectively were used to create the zero-scan image. As fewer images are used an increase in noise in the zero-scan image is clearly visible when a quadratic fit is used and less apparent when exponential and linear fits are used.

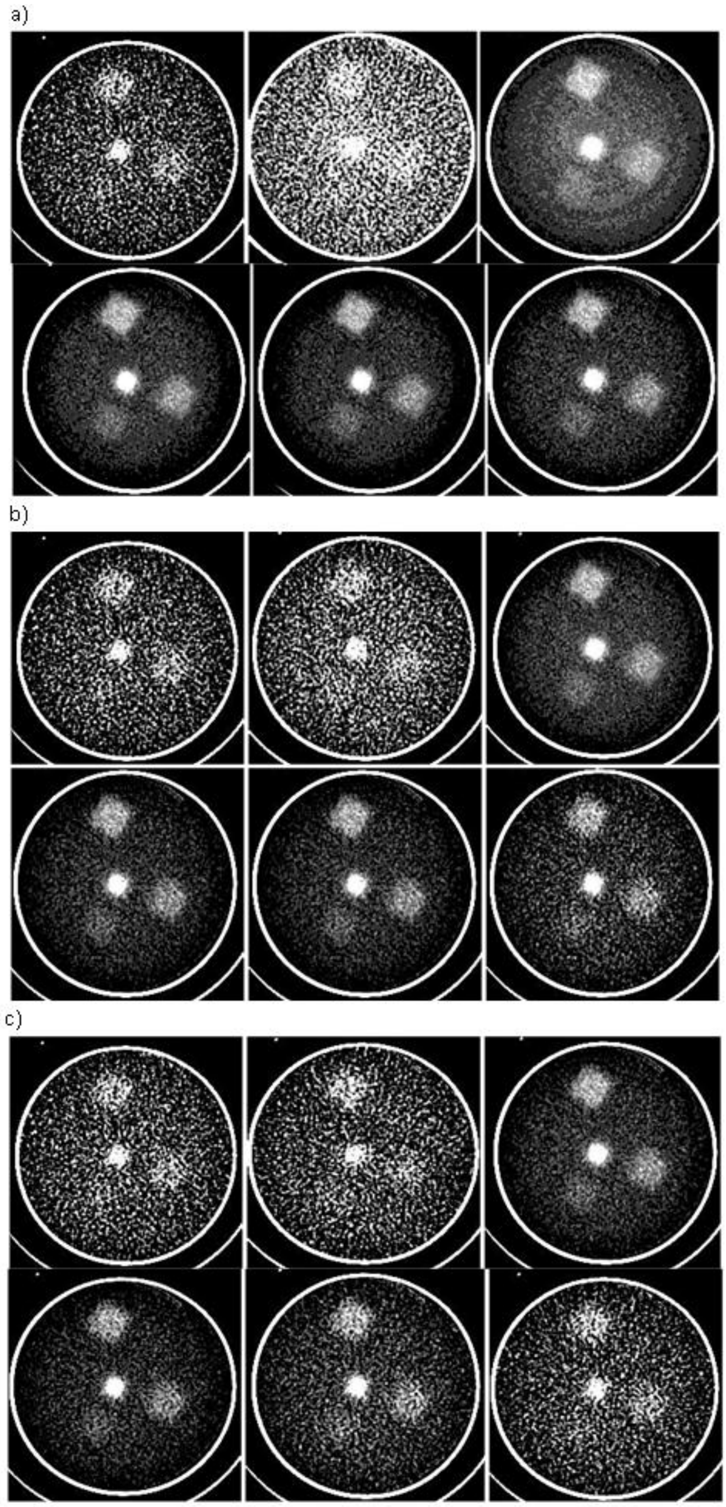

FiG. 1. a) Top left-First CT image, top center-360th CT image, Top-right-Averaged CT image. Lower left-Zero-scan image from exponential fit, Lower middle- Zero-scan image from linear fit, Lower right- Zero-scan image from quadratic fit. b) Top left-First CT image, top center-50th CT image, Top-right-Averaged CT image. Lower left- Zero-scan image from exponential fit, Lower middle- Zero-scan image from linear fit, Lower left-Zero-scan image from quadratic fit. c) Top left-First CT image, top center-16th CT image, Top-right-Averaged

CT image. Lower left- Zero-scan image from exponential fit, Lower middle- Zero-scan image from linear fit, Lower left- Zero-scan image from quadratic fit. All images are windowed to the range 19-24 HU. Profiles through the reconstructed images have been included as supplementary material.

III.B. Quantitative

Figs. 2(a) and (b) show examples of the variation in the HU values of two individual pixels throughout the acquisition of the 360 CT images. A linear fit to the data for the pixel that received 686 cGy (Fig. 2(a) has a steeper gradient (0.007±0.001)) than the linear fit to the data for the non-irradiated pixel (0.004±0.001) as shown in Fig. 2(b). This suggests that the un-irradiated gel is less sensitive to the additional dose increments delivered during the scanning process, possibly due to inhibition of the low-dose response caused by the residual presence of oxygen within the non-irradiated gel, as described by DeDeene *et al.* [31,32] Moreover, variations in manufacturing conditions may lead to different concentrations of residual oxygen between batches leading to a variations in response to the CT dose utilized in this technique. Therefore, this technique remains suitable only for relative dosimetry unless an internal absolute calibration is undertaken. [8-10]

(a)

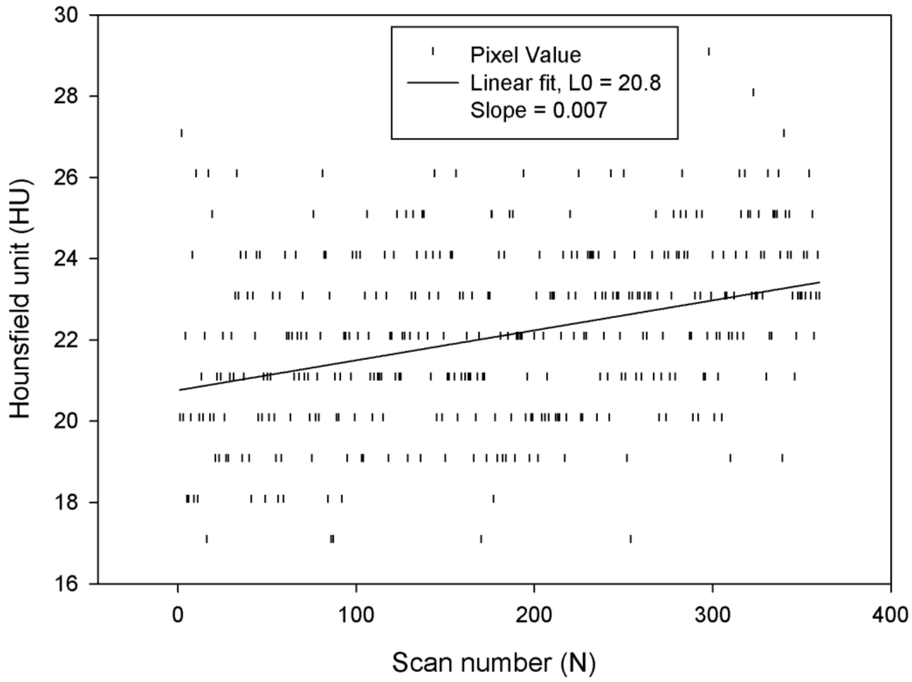
Pixel Value
Linear fit, L0 = 20.8
Slope = 0.007
Hounsfield unit (HU)
Scan number (N)
30
28
26
24
22
20
18
16
0
100
200
300
400

(b)

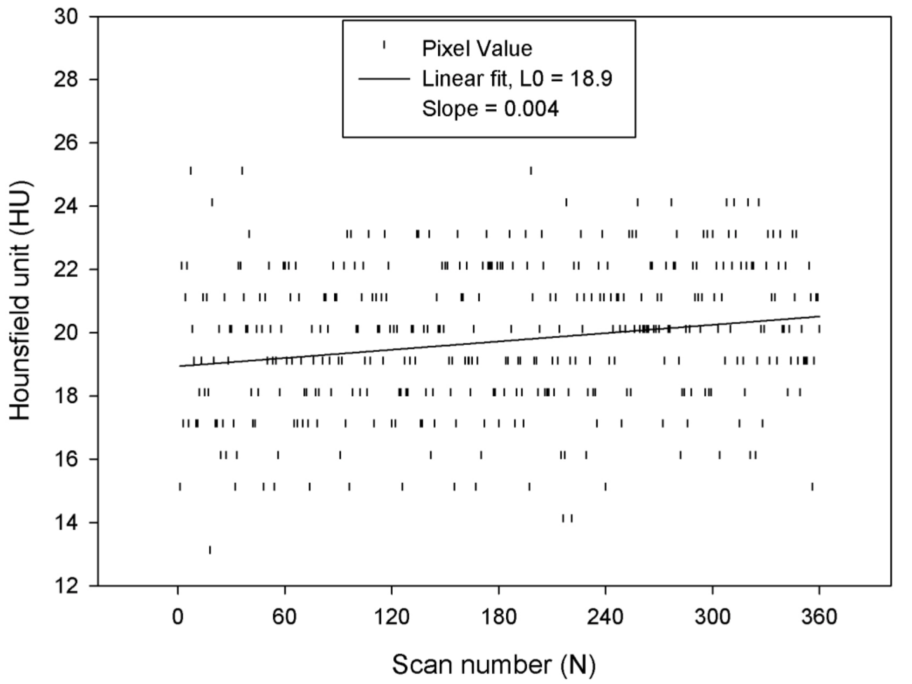
Pixel Value
Linear fit, L0 = 18.9
Slope = 0.004
Hounsfield unit (HU)
Scan number (N)
30
28
26
24
22
20
18
16
14
12
0
60
120
180
240
300
360

(c)

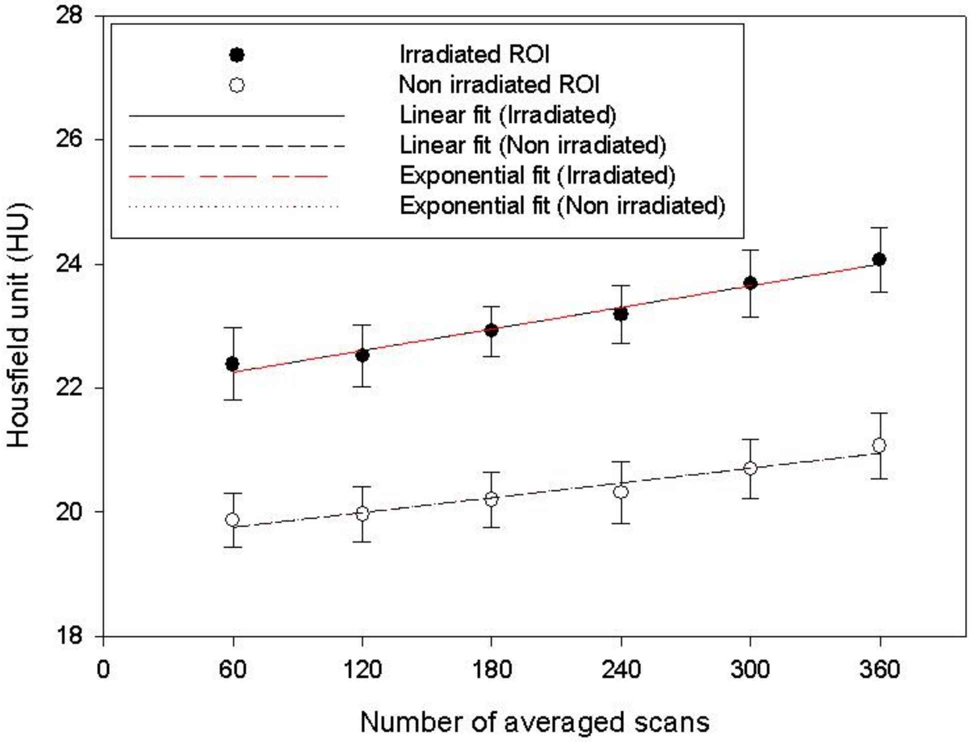

FiG. 2. (a) HU value of a single pixel inside the irradiated ROI (686 cGy), over the 360 images. (b) HU value of a single pixel outside the irradiated ROIs, over the 360 gel images c) Averaged HU values within irradiated and non irradiated ROIs (121 pixels) with linear and exponential fits. The error bars represent the mean standard deviation within the ROI.

Fig. 2(c) shows the mean pixel value of an ROI of 121 pixels calculated in the regions corresponding to irradiated and non irradiated portions of the gel, and further averaged over increasing numbers of images starting with the first raw CT/zero image. The data in Fig. 2(c) has been fitted with linear and exponential fits. Results from statistical analysis of the exponential and linear fits using 360 images are shown in Table I, which suggests that the linear and exponential fits yield similar results. Although only the data for a single pixel within the 686 cGy field is shown, similar results are noted for other pixels in this and other fields.

TABLE I. Analysis of linear and exponential fits

Fit type	Equation	Coefficients(95 % confidence bounds)	SSE	R^2
Linear Model	$f(x) = p1 * x + p2$	P1 = 0.005804 (0.00463, 0.006979) P2 = 21.91 (21.63, 22.18)	0.04509	0.9792
Exponential Model	$f(x) = a * \exp(-x/b) + c$	a = -5632 (- 2.246e+007, 2.246e+007) b = 9.701e+005 (-3.867e+009, 3.867e+009) c= 5654 (- 2.244e+007, 2.244e+007)	0.04511	0.9792

Fig. 3(a-c) shows the mean HU in each ROI in the zero-scan images of the gel, with error bars representing +/- one standard deviation from the mean for the three data sets (i.e. 360, 50 and 16 images). Since the first CT image in the series is the closest in value to the irradiated gel dosimeter prior to imaging, it is used for comparison with the other images.

a)

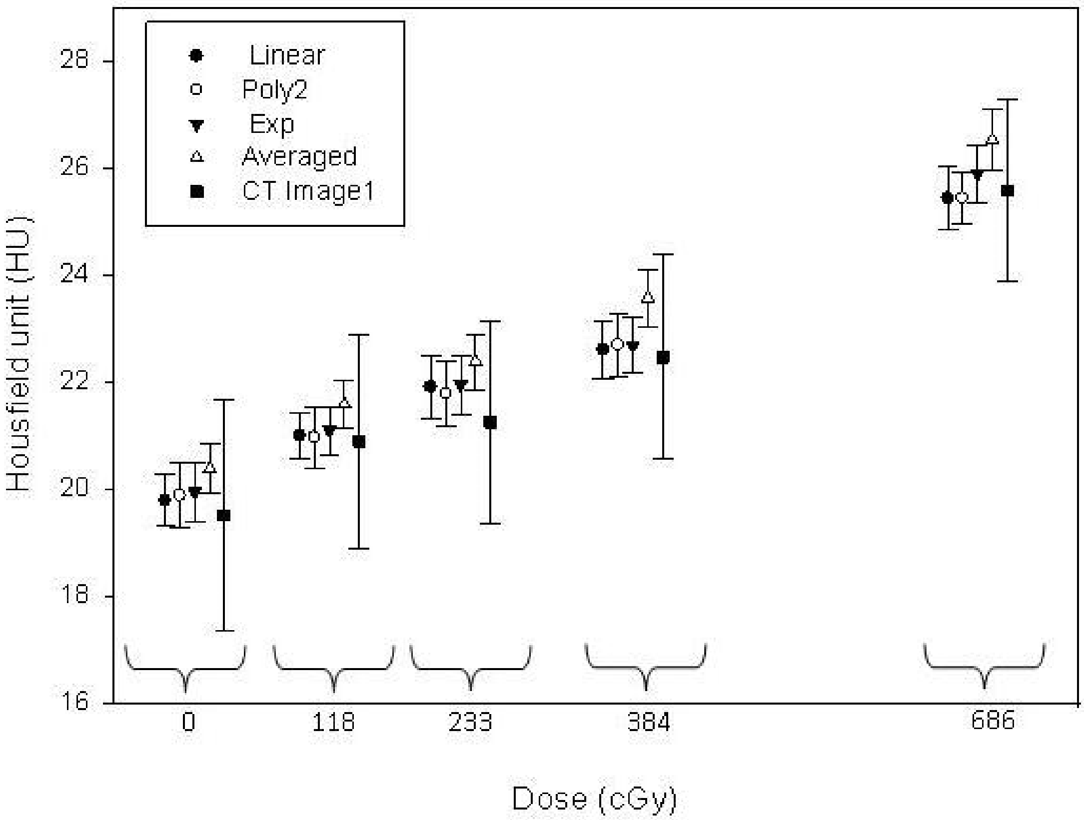
Linear
Poly2
Exp
Averaged
CT Image1
Housfield unit (HU)
28
26
24
22
20
18
16
0
118
233
384
686
Dose (cGy)

b)

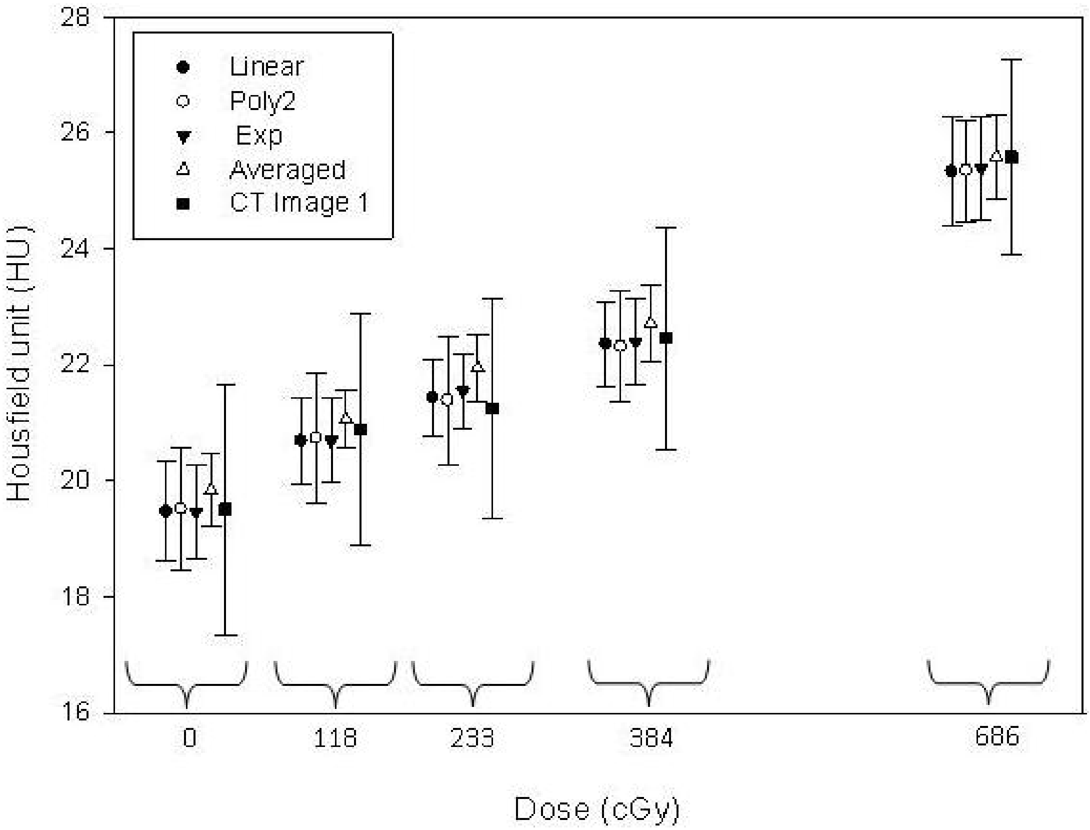
Linear
Poly2
Exp
Averaged
CT Image 1
Housfield unit (HU)
28
26
24
22
20
18
16
0
118
233
384
686
Dose (cGy)

c)

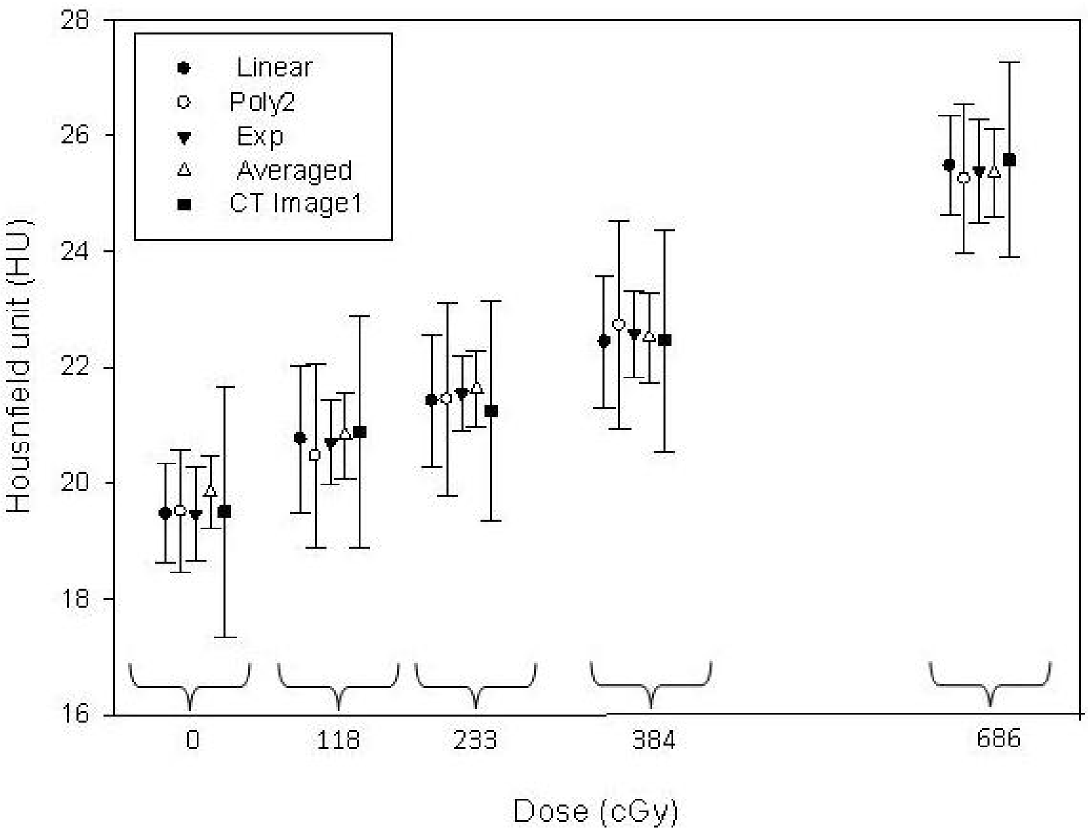

FiG.3. Plot of mean HU versus dose in cGy for all types of fit. ‘CT # 1’ refers to the fist gel image. ‘CT Averaged’ refers to the average of all gel CT images. On the x-axis the data points were shifted for visual clarity a) using 360 images b) using 50 images c) using 16 images. Error bars represent one standard deviation of the pixel values and therefore 68% confidence interval.

Fig. 3(a) shows that when all CT images are averaged together stochastic noise is reduced (as indicated by the smaller error bars on the data from the averaged scans), but the resulting mean HU values in the ROIs are consistently higher than the mean CT numbers from the corresponding ROIs in the first CT image. This suggests that although the averaging of CT images may produce more precise images, the accuracy suffers. In fact, for almost all ROIs, the mean HU value in the first CT image falls outside the error bars of the averaged image, indicating the severity of the inaccuracy of the data from the averaged image.

Fig. 3(a) shows that when using 360 CT images to create the zero-scan image, all of the fitting functions produce mean HU values in each ROI which are of a close match to the values from the first CT image. In fact, the mean ROI values from CT image 1 falls within the error bars of all corresponding zero-scan images.

In Figs. 3 (b) and 3 (c), where 50 and 16 CT images respectively are used to create the zero-scan image, there is an increase in noise compared to Fig. 3 (a) for the zero-scan images using linear, exponential and quadratic fits. The noise in the averaged image is less as compared to the fitted data however the mean value remains inaccurate indicating the deposition of the dose due to averaging. The minimum dose limit of the PAGAT gel was found to be 2.3 Gy for 0 Gy dose at 95% confidence interval using the approach reported by Trapp *et al.*[23] with a linear fit to the data.

III.C. Optimum number of scans required for reconstruction

In Fig. 4 the average % error is plotted against the number of CT images used. It clearly demonstrates that if less than 100 images are used then the error value increases; however the error remains within 0.5% if 100 or more CT images are used in the work presented here. The number of images required will naturally vary according to the uncertainty required by the user together with the CT imaging parameters (for example, see Baxter *et al.*[33]), and can be calculated by using statistical methods.

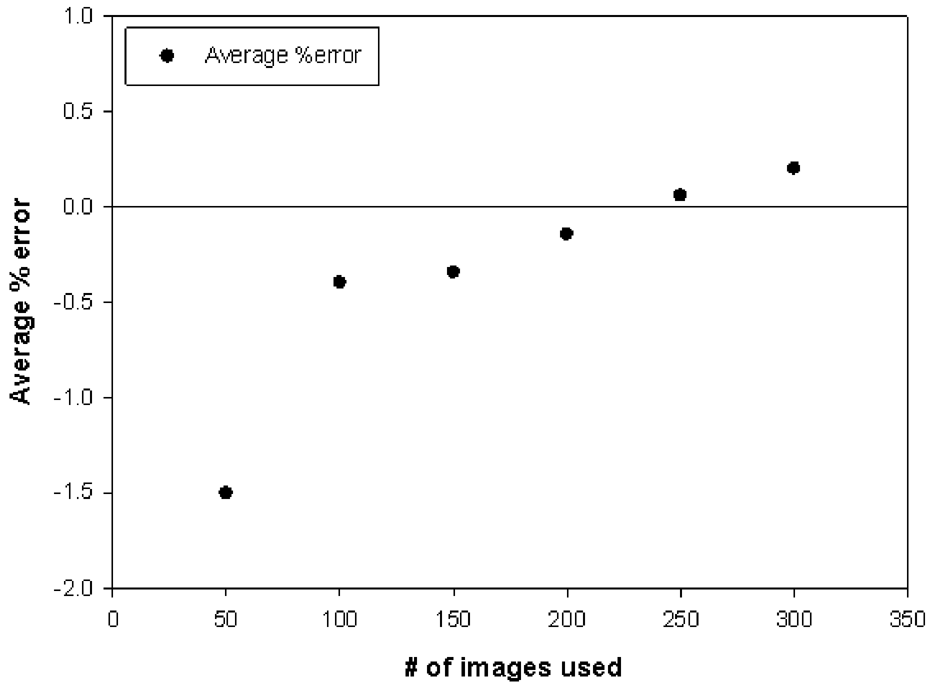

FiG.4. Plot of average % error (ROI's compared to the linear reconstructed image) versus the number of images used in image reconstruction.

IV. DISCUSSION

Reducing noise in CT imaging of gel dosimeters by averaging 360 images results in an overall increase in CT number of the final image due to the gradual increase in gel density caused by the radiation dose delivered during CT scanning. This is illustrated by the comparison between Fig. 1(a), where a visible difference is seen between images from the first and last scans, and by examination of the data in Fig. 3(a).

Comparison of the response of the non-irradiated and irradiated regions of the gel, exemplified by the different gradients of the linear fits to the individual pixel response data in Figs. 2(a) and (b) indicates that this PAGAT gel responds differently to the incremental absorption of small radiation doses (from repeated CT scanning) depending on its degree of pre-irradiation. This is additional confirmation of behaviour observed by several authors.[6,29,31,32] Some authors have shown that some polymer gel dosimeters undergo post-irradiation changes at a rate which depends upon the absorbed dose, resulting in an edge enhancement effect[6,12]. In the present work the maximum delivered dose of 686 cGy is below that shown to produce measurable changes in the 24 hour irradiation-to-imaging time; however if this technique is used with larger doses then earlier imaging may be required to ensure accuracy.

Fitting a function to the pixel data and using this to evaluate a zero-scan image substantially reduces image noise, while providing accurate measurements (see Figs. 2 and 3). Fitting the exponential fit does not result in any additional advantage in analysing CT images according to the method described here as the level of extra dose delivered via CT scanning is low and the gel's subsequent response shows no obvious non-linearity. When analysing CT data by producing a zero-scan image, data shown in Fig. 3 suggest that the use of a simple, linear fitting relationship is suitably accurate in situations where a user does not have access to exponential fitting software.

The technique presented here can be accompanied by further techniques for noise improvement including image filtering[24,27,28],However the application of a particular filtering strategy is dependent on the nature of the dose distribution and the noise present in the original CT data. Reduction of noise by averaging the CT images[20,21] will result in inaccuracies as evident from Fig. 3.

The data presented here represents results from specific scanning parameters on a specific scanner and gel dosimeter. If parameters are varied the technique presented here will continue to work if the gel dosimeter chosen changes CT number with dose. For example, using a smaller slice thickness will increase the stochastic noise in each acquisition, thus increasing the noise in Fig. 2, however providing a large enough sample size is acquired the fitted function (and therefore intercept) will not significantly alter. Similarly, using a more sensitive gel dosimeter [34,35]may reduce the number of images required for suitable results using this technique, and future work beyond the scope of this paper will refine this technique.

V. CONCLUSION

A simple method has been proposed for improving the image quality of polymer gel dosimeters imaged with x-ray CT. It has been shown that a simple analysis of the increase in HU with repeated imaging can be used to produce an accurate, low-noise 'zero-scan' image of the gel. The zero-scan image prediction method described here has been shown to be capable of improving the precision while maintaining the accuracy of a two-dimensional single-slice CT image of a gel sample irradiated to a range of doses. Use of multi-slice or cone-beam CT modalities to provide repeated three-dimensional CT scans of the gel would allow this method to be applied in three dimensions, without the measured dose being compromised by scattering effects from adjacent slices.

Acknowledgments

The authors would like to acknowledge the help of Chris Poole in the preparation of the gel dosimeters.

[a] Conflict of interest notification. The authors report no actual or potential conflict of interests.

[1]C . Baldock, Y. De Deene, S. Doran, G. Ibbot, A. Jirasek, M. Lepage, K. B. McAuley ,M. Oldham, L. J. Schreiner, "Polymer gel dosimetry," Phys .Med. Biol. **55**, R1-R63 (2010).

[2]G. Massillon-JL, R. Minniti, M. G. Mitch, M. J. Maryanski, C. G. Soares, "The use of gel dosimetry to measure the 3D dose distribution of a 90 Sr/ 90 Y intravascular brachytherapy seed," Phys .Med. Biol. **54**, 1661-1672 (2009).

[3]S. J. Doran, T. Brochard, J. Adamovics, N. Krstajic, E. Br¨auer-Krisch, "An investigation of the potential of optical computed tomography for imaging of synchrotron-generated x-rays at high spatial resolution, " Phys. Med. Biol. **55**, 1531-1547 (2010).

[4]T. Olding, O. Holmes, L. J. Schreiner, Cone beam optical computed tomography for gel dosimetry I: scanner characterization," Phys. Med. Biol. **55**, 2819-2840 (2010).

[5]X. Ding, J. Olsen, R. Best, M. Bennett, I. McGowin, J. Dorand, K. Link, J. D. Bourland, "High resolution polymer gel dosimetry for small beam irradiation using a 7T micro-MRI scanner, " J. Phys: Conf. Series **250**, 01204 (2010).

[6]G. Massillon-JL, R. Minniti, C. G. Soares, M. J. Maryanski, S. Robertson, "Characteristics of a new polymer gel for high-dose gradient dosimetry using a micro optical CT scanner," Appl. Radiat. Isot. **68**, 144-154 (2010).

[7]G. Massillon-JL, R. Minniti, M. G. Mitch, C. G. Soares, R. A. Hearn, "High-resolution 3D dose distribution measured for two low-energy x-ray brachytherapy seeds: 125I and 103Pd," Rad. Meas. **46**, 238-243 (2011).

[8]N. M. Tremblay, V.Hubert-Tremblay, R. Bujold, L. Beaulieu' M. Lepage, "Improvement in the accuracy of polymer gel dosimeters using scintillating fibers," J. Phys: Conf. Series **250**, 012076 (2010).

[9]C. Poole, J. V. Trapp, J. Kenny, T. Kairn, K. Williams, M. Taylor, R. Franich, C. Langton, "A hybrid radiation detector for simultaneous spatial and temporal dosimetry," (In Press, Australas. Phys. Eng. Sci. Med.)

[10]J.V. Trapp, T. Kairn, S. Crowe and A. Fielding, "Internal calibration of gel dosimeters: A feasibility study" J. Phys: Conf. Ser. **164,** 012014 (2009).

[11]M. J. Maryanski, J. C. Gore, R. P. Kennan, R. J. Schulz, "NMR relaxation enhancement in gels polymerized and cross-linked by ionizing radiation: a new approach to 3D dosimetry by MRI ," Magn. Reson. Imaging **11**, 253-258 (1993).

[12]M. J. Maryanski, R. J. Schulz, G. S. Ibbott, J. C. Gatenby, J. Xie, D. Horton, J. C. Gore, "Magnetic resonance imaging of radiation dose distributions using a polymer-gel dosimeter," Phys. Med. Biol. **39**, 1437–1455 (1994).

[13]G. S. Ibbott, M. J. Maryanski, P. Eastman, S. D. Holcomb, Y. Zhang, R. G. Avison, M . Sanders, J. C. Gore, "Three-dimensional visualization and measurement of conformal dose distributions using magnetic resonance imaging of BANG polymer gel dosimeters," Int. J. Radiat. Oncol. Biol. Phys. **38**, 1097-1103 (1997).

[14]Y. De Deene, C. De Wagter, B. Van Duyse, S. Derycke, W. De Neve, E. Achten, "Three-dimensional dosimetry using polymer gel and magnetic resonance imaging applied to the verification of conformal radiation therapy in head-and-neck cancer," Radiother. Oncol. **48**, 283–291 (1998).

[15]J. C. Gore, M. Ranade, M. J. Maryanski, R. J. Schulz, "Radiation dose distributions in three dimensions from tomographic optical density scanning of polymer gels: I. Development of an optical scanner," Phys .Med. Biol. **41**, 2695-2704 (1996).

[16]M. J. Maryanski, Y. Z. Zastavker, J. C. Gore, "Radiation dose distributions in three dimensions from tomographic optical density scanning of polymer gels: II. Optical properties of the BANG polymer gel," Phys. Med. Biol. **41**, 2705–2717 (1996).

[17]M. L. Mather, A. K. Whittaker, C. Baldock, "Ultrasound evaluation of polymer gel dosimeters," Phys .Med. Biol. **47**, 1449 (2002).

[18]N. Krstajic, S. Doran, "Initial characterization of fast laser scanning optical CT apparatus for 3-D dosimetry," J. Phys: Conf. Series **164**, 012022 (2009).

[19]M. Oldham, "Optical CT scanning of polymer gels," DOSGEL 2006. Sherbrooke editors: (2006).

[20]M. Hilts, C. Audet, C. Duzenli and A. Jirasek, "Polymer gel dosimetry using x-ray computed tomography: a feasibility study," Phys. Med. Biol. **45**, 2559-2571 (2000).

[21]J. V. Trapp, S. Å. J. Bäck, M. Lepage, G. Michael and C. Baldock, “An experimental study of the dose response of polymer gel dosimeters imaged with x-ray computed tomography,” Phys .Med. Biol. **46**, 2939-2951 (2001).

[22] J. V. Trapp, G. Michael, Y. De Deene and C. Baldock, “Attenuation of diagnostic energy photons by polymer gel dosimeters,” Phys. Med. Biol. **47**, 4247-4258 (2002).

[23]J. V. Trapp, G. Michael, P. M. Evans, C. Baldock, M. O. Leach and S. Webb, “Dose resolution in gel dosimetry: effect of uncertainty in the calibration function,” Phys. Med. Biol. **49**, N139-N146 (2004).

[24] M. Hilts and C. Duzenli, “Image filtering for improved dose resolution in CT polymer gel dosimetry,” Med. Phys. **31**, 39-49 (2004).

[25] C. Audet, M. Hilts ,A. Jirasek, C. Duzenli “CT gel dosimetry technique: Comparison of a planned and measured 3D stereotactic dose volume,” J. Appl. Clin. Med. Phys. **3**, 110-118 (2002).

[26]J. V. Trapp, “Imaging and radiation interactions of polymer gel dosimeters,” PhD thesis. (Brisbane: QUT), (2003).

[27]A . Jirasek, Q. Matthews, M. Hilts, G. Schulz, M. W. Blades and R. F. B. Turner, “Investigation of a 2D two-point maximum entropy regularization method for signal-to-noise ratio enhancement: application to CT polymer gel dosimetry,” Phys .Med. Biol. **51**, 2599-2617 (2006).

[28]M. Hilts and A . Jirasek, “Adaptive mean filtering for noise reduction in CT polymer gel dosimetry,” Med. Phys.**35**, 344-355 (2008).

[29]A. J. Venning, B. Hill, S. Brindha, B. J. Healy and C. Baldock, “Investigation of the PAGAT polymer gel dosimeter using magnetic resonance imaging,” Phys .Med. Biol. **50**, 3875-3888 (2005).

[30]S. Kohei, J. B. Moorrees, C. M. Langtom and J. V. Trapp, “An investigation of the pre-irradiation temporal stability of PAGAT gel dosimeter,” In: IC3DDose, 6th International Conference on 3D Radiation Dosimetry, ed M Oldham (Hilton Head Island, SC, USA: Duke University Medical Center), (2010).

[31]Y. De Deene, P. Hanselaer, C. De Wagter, E. Achten and W. De Neve, “An investigation of the chemical stability of a monomer/polymer gel dosimeter,” Phys. Med. Biol. **45**, 859-878 (2000).

[32]Y. De Deene, C. Hurley, A. J. Venning, K. Vergote, M. Mather, B. J. Healy and C. Baldock, “A basic study of some normoxic polymer gel dosimeters,” Phys. Med. Biol. **47**, 3441-3463 (2002).

[33]P. Baxter, A. Jirasek, M. Hilts, "X-ray CT dose in normoxic polyacrylamide gel dosimetry," Med. Phys. **34**, 1934–1943 (2007).

[34]Koeva, T. Olding, A. Jirasek, L.J. Schreiner and K.B. McAuley, "Preliminary investigation of the NMR, optical and X-ray CT dose-response of polymer gel dosimeters incorporating cosolvents to improve dose sensitivity," Phys. Med. Biol. **54**, 2779-2790 (2009).

[35]M. Hilts and A . Jirasek, K. B. McAuely, "Polymer gel dosimeters with enhanced sensitivity for use in x-ray CT polymer gel dosimetry," Phys. Med. Biol. **55**, 5269-5281 (2010).